

# Rovibrational levels of helium hydride ion

Krzysztof Pachucki\*

*Faculty of Physics, University of Warsaw,  
Hoża 69, 00-681 Warsaw, Poland*

Jacek Komasa†

*Faculty of Chemistry, A. Mickiewicz University,  
Grunwaldzka 6, 60-780 Poznań, Poland*

(Dated: November 5, 2012)

## Abstract

Dissociation energy ( $D_0$ ) of rovibrational levels of  $^4\text{HeH}^+$  has been predicted theoretically to the accuracy of the order of  $0.01\text{ cm}^{-1}$ . The calculations take into account adiabatic and non-adiabatic corrections as well as relativistic and QED effects. For the ground rovibrational level  $D_0 = 14874.213(10)\text{ cm}^{-1}$  and it differs by several tens of the inverse centimeter from previous theoretical estimations. For a collection of about fifty transition energies measured between dipole connected levels the difference between theory and experiment is of the order of hundredths of  $\text{cm}^{-1}$  or less.

---

\*Electronic address: krp@fuw.edu.pl

†Electronic address: komasa@man.poznan.pl

## I. INTRODUCTION

Formed by the most abundant elements, the hydrohelium plays an important role in astrophysics. According to the standard Big Bang model, the helium hydride ion  $\text{HeH}^+$  is the first molecule, along with  $\text{He}_2^+$ , formed in the Universe [1, 2] and its significance in the early Universe chemistry cannot be overestimated [3]. Because of its low abundance, caused by processes competitive to its formation,  $\text{HeH}^+$  is expected to be difficult to observe. Several rotational lines have been selected as candidates for such observations [4, 5]. Although  $\text{HeH}^+$  is expected to be observable in a variety of astrophysical environments [6–9], no unequivocal detection has been reported to date.  $\text{HeH}^+$  is present in helium-hydrogen plasma produced in a variety of experiments and most of the spectroscopic data available today originates from the laboratory measurements. Large permanent dipole moment of  $\text{HeH}^+$  enables acquisition of highly accurate spectra in the gas phase. The knowledge of the rovibrational spectrum of the bound and quasi-bound states allows an evaluation of cross sections for spontaneous and stimulated processes of formation of  $\text{HeH}^+$  in the interstellar space [10]. Such cross sections, in turn, enable prediction of pertinent reaction rates indispensable for understanding the reactions mechanisms [11] and for verification of cosmological models.

Interestingly, experimental and theoretical studies of  $^3\text{HeT}^+$  [12] at that time were motivated by the neutrino mass measurements. Experimental data for other isotopomers are available in literature [13–15], hence the isotopic substitution effect can be studied. Such data have been used by Coxon and Hajigeorgiu [16] in solving an inverse rovibrational problem, i.e. to construct an empirical Born-Oppenheimer (BO) interaction potential. Their estimated interaction energy at the equilibrium of the BO potential ( $16\,456.24 \pm 0.1 \text{ cm}^{-1}$ ) is by  $0.83 \text{ cm}^{-1}$  smaller than the exact value of Ref. [17].

$\text{HeH}^+$  is a relatively simple heteronuclear molecular ion, isoelectronic with  $\text{H}_2$ , which makes it of a fundamental significance from the theoretical point of view. There is extensive literature reporting quantum chemical calculations on this system. Apart from correlated methods based on the one-electron approximation [18–20], more sophisticated methods of explicitly correlated wave functions expanded in the James-Cooledge (JC) or gaussian (ECG) basis have been employed. Early calculations were limited to very short expansions and a few internuclear distances  $R$  [21–23]. The first accurate calculations of the Born-Oppenheimer (BO) energy curve can be attributed to Wolniewicz [24]. He applied the obtained wave

function to study a formation of  $\text{HeH}^+$  from HT molecule through the  $\beta$  decay process. Ten years later, Kołos and Peek [25, 26] extended the BO calculations to long distances, which enabled studies of quasi-bound energy levels. An important step forward has been made by Bishop and Cheung [27] who have significantly improved the accuracy of previous results and additionally evaluated the adiabatic correction to the BO curve. A few years ago, accurate nonadiabatic-relativistic energies for rotationless levels have been obtained using ECG functions by Stanke *et al.* [28]. Very recently, a state-of-the-art BO potential has been obtained with relative accuracy of  $10^{-12}$  [17].

Spectroscopists claim that, "the spectroscopic measurements are typically four orders of magnitude more precise than the theoretical spectra!" [29]. The exceptions are the two electron diatomic molecules, such as  $\text{H}_2$  and  $\text{HeH}^+$ . We report here on results obtained using the methodology applied successfully to hydrogen molecule and its isotopomers [30–33]. Those theoretical predictions have been verified by subsequent experiments [29, 33–39].

Our goal is to supply a theoretically predicted spectrum of the bound states of  $\text{HeH}^+$  with the highest possible accuracy achievable within the present day stage of theoretical and computational methods. Such a full energy spectrum can be helpful in selection of those astrophysical objects at which  $\text{HeH}^+$  can potentially be detected.

## II. METHODOLOGY

In the frames of the so-called nonrelativistic quantum electrodynamics (NRQED) [40–42], relativistic and QED effects are included in successive terms of the perturbation series

$$E = E^{(0)} + \alpha^2 E^{(2)} + \alpha^3 E^{(3)} + \alpha^4 E^{(4)} + \dots \quad (1)$$

whereas the nonrelativistic component  $E^{(0)}$  of the total energy is evaluated using the recently developed nonadiabatic perturbation theory (NAPT) [43, 44].

A short account of the underpinning theory will be presented below. More details will be given only on these items which are new or specific to  $\text{HeH}^+$ . Atomic units will be used throughout unless explicitly stated.

## A. Nonrelativistic Hamiltonian

The nonrelativistic Hamiltonian of an  $N$ -electron diatomic molecule entering the Schrödinger equation

$$H \Psi = E \Psi \quad (2)$$

can be split into the electronic and nuclear parts

$$H = H_{\text{el}} + H_{\text{n}}. \quad (3)$$

The former includes the kinetic energy of the electrons and the Coulomb interactions between all the particles

$$H_{\text{el}} = -\frac{1}{2} \sum_{a=1}^N \nabla_a^2 + V, \quad (4)$$

with

$$V = -Z_A \sum_{a=1}^N \frac{1}{r_{aA}} - Z_B \sum_{a=1}^N \frac{1}{r_{aB}} + \sum_{a=1}^{N-1} \sum_{b=a+1}^N \frac{1}{r_{ab}} + \frac{Z_A Z_B}{R}. \quad (5)$$

The notation employed to describe a location of particles is defined in Figure 1.

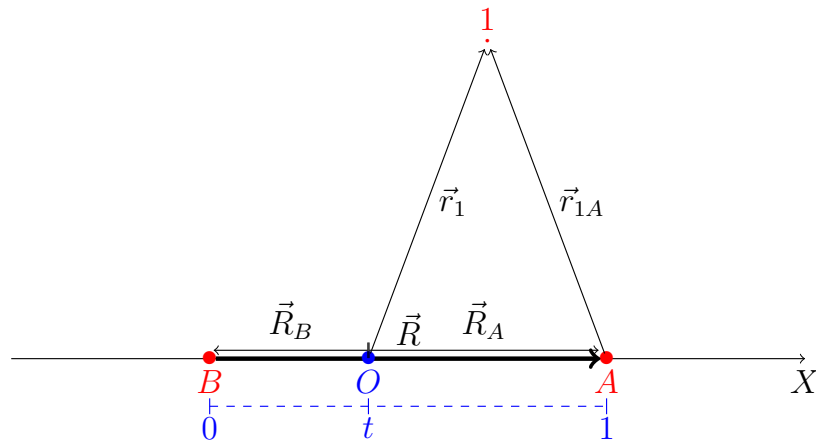


FIG. 1: Vectors defining the geometric structure of the molecule.  $A$  and  $B$  are the hydrogen ( $Z_A = 1$ ) and helium ( $Z_B = 2$ ) nucleus positions, respectively.  $O$  is the location of the arbitrarily chosen origin of the coordinate system.

Before we write down explicitly the nuclear Hamiltonian of a diatomic molecule, we introduce a parameter  $t$  which specifies the origin,  $O$ , of the molecule-fixed coordinate system.

As shown in Figure 1,  $t$  is a fraction of the internuclear distance measured from the 'left' nucleus, so that the nuclear positions are:

$$\vec{R}_A = (1-t)\vec{R} \quad \text{and} \quad \vec{R}_B = -t\vec{R} \quad (6)$$

and the vectors pointing at the electron 1 from the nuclei are

$$\vec{r}_{1A} = \vec{r}_1 - (1-t)\vec{R} \quad \text{and} \quad \vec{r}_{1B} = \vec{r}_1 + t\vec{R}. \quad (7)$$

With the nuclear masses  $M_A$  and  $M_B$  ( $M = M_A + M_B$ ), and the nuclear reduced mass  $\mu_n = (1/M_A + 1/M_B)^{-1}$ , we can write [45]

$$H_n = -\frac{1}{2\mu_n}\nabla_R^2 - \frac{1}{2}\left(\frac{t^2}{M_A} + \frac{(1-t)^2}{M_B}\right)\nabla_{\text{el}}^2 + \left(\frac{t}{M_A} - \frac{1-t}{M_B}\right)\vec{\nabla}_R \cdot \vec{\nabla}_{\text{el}}. \quad (8)$$

Here we have introduced a shorthand notation  $\vec{\nabla}_{\text{el}} = \sum_{a=1}^N \vec{\nabla}_a$ . Additionally, we define a new differential operator

$$\tilde{\nabla} = \vec{\nabla}_R - \left(t - \frac{M_A}{M}\right)\vec{\nabla}_{\text{el}} \quad (9)$$

which has an important feature—its action on the electronic wave function  $\varphi_{\text{el}}$  is  $t$ -invariant. We note, that if  $t = \frac{M_A}{M}$  i.e. the origin is selected at the center of nuclear mass (CNM), the two above equations simplify—the last term in both cases vanishes. Finally, using the introduced abbreviations, we arrive at the following compact form of the  $t$ -dependent nuclear Hamiltonian

$$H_n = -\frac{1}{2\mu_n}\tilde{\nabla}^2 - \frac{1}{2M}\nabla_{\text{el}}^2. \quad (10)$$

## B. Adiabatic approximation

Our zero-order ansatz is in the form of a product of electronic and nuclear wave functions

$$\phi_a(\vec{r}, \vec{R}) = \phi_{\text{el}}(\vec{r}) \chi(\vec{R}), \quad (11)$$

the former being a solution to the electronic Schrödinger equation with the clamped nuclei Hamiltonian (4)

$$H_{\text{el}}\varphi_{\text{el}} = \mathcal{E}_{\text{el}}\varphi_{\text{el}} \quad (12)$$

and the latter—to the nuclear Schrödinger equation

$$\left[ -\frac{\nabla_R^2}{2\mu_n} + \mathcal{E}_{\text{el}}(R) + \mathcal{E}_a(R) \right] \chi(\vec{R}) = E_a \chi(\vec{R}), \quad (13)$$

with the adiabatic correction

$$\begin{aligned} \mathcal{E}_a &= \langle \varphi_{\text{el}} | H_n | \varphi_{\text{el}} \rangle_{\text{el}} \\ &= -\frac{1}{2\mu_n} \langle \varphi_{\text{el}} | \tilde{\nabla}^2 | \varphi_{\text{el}} \rangle_{\text{el}} - \frac{1}{2M} \langle \varphi_{\text{el}} | \nabla_{\text{el}}^2 | \varphi_{\text{el}} \rangle_{\text{el}} \end{aligned} \quad (14)$$

included in the potential for the movement of the nuclei.

### C. Nonadiabatic effects

The nonadiabatic effects can be taken into account using the perturbation theory (NAPT) introduced in Ref. 43 and developed in Ref. 44. According to this theory the leading order correction to energy of a molecular level is given by

$$E_{\text{na}}^{(2)} = \left\langle \varphi_{\text{el}} \chi \left| H_n \frac{1}{(\mathcal{E}_{\text{el}} - H_{\text{el}})'} H_n \right| \varphi_{\text{el}} \chi \right\rangle. \quad (15)$$

Alternatively, the level energy can be obtained as a solution to the nonadiabatic radial Schrödinger equation

$$\begin{aligned} \left[ -\frac{1}{R^2} \frac{\partial}{\partial R} \frac{R^2}{2\mu_{\parallel}(R)} \frac{\partial}{\partial R} + \frac{J(J+1)}{2\mu_{\perp}(R)R^2} + \mathcal{Y}(R) \right] \tilde{\chi}_J(R) \\ = E \tilde{\chi}_J(R), \end{aligned} \quad (16)$$

where

$$\mathcal{Y}(R) = \mathcal{E}_{\text{el}}(R) + \mathcal{E}_a(R) + \delta\mathcal{E}_{\text{na}}(R). \quad (17)$$

The solution  $\tilde{\chi}_J(R)$  is a radial part of  $\chi$  for a given angular momentum  $J$ . The energy  $E$  includes the adiabatic energy  $E_a$ , the second order nonadiabatic correction  $E_{\text{na}}^{(2)}$ , and an admixture of higher order corrections.

In analogy with the original approach [43, 44], the  $R$ -dependent reduced nuclear masses  $\mu_{\parallel}(R)$  (vibrational) and  $\mu_{\perp}(R)$  (rotational) are defined through the potentials  $\mathcal{W}(R)$ .

$$\frac{1}{2\mu_{\parallel}(R)} = \frac{1}{2\mu_n} + \mathcal{W}_{\parallel}(R), \quad (18)$$

$$\frac{1}{2\mu_{\perp}(R)} = \frac{1}{2\mu_n} + \mathcal{W}_{\perp}(R). \quad (19)$$

These, however, differ from their original counterparts in using  $\vec{\nabla}$  operator rather than  $\vec{\nabla}_R$

$$\mathcal{W}_{\parallel}(R) = \frac{1}{\mu_n^2} \frac{1}{R^2} \left\langle R^i \tilde{\nabla}^i \varphi_{\text{el}} \left| \frac{1}{(\mathcal{E}_{\text{el}} - H_{\text{el}})'} \right| R^j \tilde{\nabla}^j \varphi_{\text{el}} \right\rangle_{\text{el}}, \quad (20)$$

$$\mathcal{W}_{\perp}(R) = \frac{1}{\mu_n^2} \frac{1}{2} \left( \delta^{ij} - \frac{R^i R^j}{R^2} \right) \left\langle \tilde{\nabla}^i \varphi_{\text{el}} \left| \frac{1}{(\mathcal{E}_{\text{el}} - H_{\text{el}})'} \right| \tilde{\nabla}^j \varphi_{\text{el}} \right\rangle_{\text{el}}. \quad (21)$$

Referring again to the original formulation, we recall here that the nonadiabatic correction to the BO potential is

$$\delta\mathcal{E}_{\text{na}}(R) = \mathcal{U}(R) + \left( \frac{2}{R} + \frac{\partial}{\partial R} \right) (\mathcal{V}(R) + \delta\mathcal{V}(R)). \quad (22)$$

The three functions of  $R$  referenced above are defined as follows

$$\mathcal{U}(R) = \left\langle H_n \varphi_{\text{el}} \left| \frac{1}{(\mathcal{E}_{\text{el}} - H_{\text{el}})'} \right| H_n \varphi_{\text{el}} \right\rangle_{\text{el}}, \quad (23)$$

$$\mathcal{V}(R) = -\frac{1}{\mu_n} \frac{1}{R} \left\langle H_n \varphi_{\text{el}} \left| \frac{1}{(\mathcal{E}_{\text{el}} - H_{\text{el}})'} \right| R^i \tilde{\nabla}^i \varphi_{\text{el}} \right\rangle_{\text{el}}, \quad (24)$$

$$\delta\mathcal{V}(R) = -\frac{1}{2\mu_n^2} \frac{d\mathcal{E}_{\text{el}}(R)}{dR} \left\langle R^i \tilde{\nabla}^i \varphi_{\text{el}} \left| \frac{1}{[(\mathcal{E}_{\text{el}} - H_{\text{el}})']^2} \right| R^j \tilde{\nabla}^j \varphi_{\text{el}} \right\rangle_{\text{el}}. \quad (25)$$

### III. RELATIVISTIC AND QED POTENTIALS

In accordance with the expansion (1), the nonadiabatic potential of Eq. (17) can be further augmented by the relativistic and QED potentials

$$\begin{aligned} \mathcal{Y}(R) &= \mathcal{E}_{\text{el}}(R) + \mathcal{E}_a(R) + \delta\mathcal{E}_{\text{na}}(R) \\ &+ \mathcal{E}^{(2)}(R) + \mathcal{E}^{(3)}(R) + \mathcal{E}^{(4)}(R) + \mathcal{E}_{\text{fs}}(R). \end{aligned} \quad (26)$$

The relativistic ( $\alpha^2$ ) effects are described by an expectation value of the Breit-Pauli Hamiltonian

$$\begin{aligned} \mathcal{E}^{(2)}(R) &= \\ &\alpha^2 \left\langle \phi_{\text{el}} \left| -\frac{1}{8} \sum_a p_a^4 + \frac{\pi}{2} \sum_{a,A} Z_A \delta(\vec{r}_{aA}) + \pi \sum_{a<b} \delta(\vec{r}_{ab}) \right. \right. \\ &\quad \left. \left. - \frac{1}{2} \sum_{a<b} \left( \vec{p}_a \frac{1}{r_{ab}} \vec{p}_b + \vec{p}_a \cdot \vec{r}_{ab} \frac{1}{r_{ab}^3} \vec{r}_{ab} \cdot \vec{p}_b \right) \right| \phi_{\text{el}} \right\rangle_{\text{el}}. \end{aligned} \quad (27)$$

Additionally, we consider a small effect of the finite nuclear size given by

$$\mathcal{E}_{\text{fs}}(R) = \frac{2\pi}{3}\alpha^2 \sum_{a,A} Z_A \frac{r_{\text{ch}}^2(A)}{\lambda_C^2} \langle \varphi_{\text{el}} | \delta(\vec{r}_{aA}) | \varphi_{\text{el}} \rangle_{\text{el}}, \quad (28)$$

where  $\lambda_C = 386.15926459$  fm is the electron Compton wavelength over  $2\pi$  and where the square root mean nuclear charge radii are  $r_{\text{ch}}(\text{H}) = 0.84184(67)$  fm and  $r_{\text{ch}}(^4\text{He}) = 1.681(4)$  fm [46]. However, this effect turns out to be insignificant in comparison with overall accuracy we accomplished for the relativistic correction, so we have dropped out the  $\mathcal{E}_{\text{fs}}$  potential in Eq. (26).

The leading order ( $\alpha^3$ ) QED correction is given by

$$\begin{aligned} \mathcal{E}^{(3)}(R) = \alpha^3 \sum_{a<b} \left\{ \left[ \frac{164}{15} + \frac{14}{3} \ln \alpha \right] \langle \varphi_{\text{el}} | \delta(\vec{r}_{ab}) | \varphi_{\text{el}} \rangle_{\text{el}} \right. \\ \left. - \frac{7}{6\pi} \left\langle \varphi_{\text{el}} \left| \frac{1}{r_{ab}^3} \right| \varphi_{\text{el}} \right\rangle_{\text{el}} \right\} \\ + \alpha^3 \sum_{a,A} \left[ \frac{19}{30} - 2 \ln \alpha - \ln k_0(R) \right] \frac{4Z_A}{3} \langle \varphi_{\text{el}} | \delta(\vec{r}_{aA}) | \varphi_{\text{el}} \rangle_{\text{el}}. \end{aligned} \quad (29)$$

This formula includes the so-called Bethe logarithm  $\ln k_0$  defined as

$$\begin{aligned} \ln k_0(R) = \\ \frac{\langle \varphi_{\text{el}} | \sum_{a=1}^N \vec{p}_a (H_{\text{el}} - \mathcal{E}_{\text{el}}) \ln[2(H_{\text{el}} - \mathcal{E}_{\text{el}})] \sum_b \vec{p}_b | \varphi_{\text{el}} \rangle}{\langle \varphi_{\text{el}} | \sum_{a=1}^N \vec{p}_a (H_{\text{el}} - \mathcal{E}_{\text{el}}) \sum_b \vec{p}_b | \varphi_{\text{el}} \rangle}. \end{aligned} \quad (30)$$

So far, calculation of the higher order ( $\alpha^4$ ) QED corrections for a two electron molecule is infeasible. However, the experience gained with two electron atoms [42] validates the assumption that this correction can be well estimated by its dominating component, the so-called one-loop term  $\mathcal{E}^{(4)}(R) \approx \mathcal{E}_{\text{one-loop}}^{(4)}(R)$ , which can be readily evaluated from the formula

$$\begin{aligned} \mathcal{E}_{\text{one-loop}}^{(4)}(R) = \\ \pi \alpha^4 \left( \frac{427}{96} - \ln 4 \right) \sum_{a,A} Z_A \langle \varphi_{\text{el}} | \delta(\vec{r}_{aA}) | \varphi_{\text{el}} \rangle_{\text{el}}. \end{aligned} \quad (31)$$

#### IV. NUMERICAL ASPECTS, RESULTS AND DISCUSSION

The following physical constants [47] were used in the present calculations: the proton mass  $M_p = 1836.15267247$ , the  $\alpha$  particle mass  $M_\alpha = 7294.2995365$ , the conversion factor  $1 \text{ hartree} = 219474.6313705 \text{ cm}^{-1}$ , and the fine-structure constant  $\alpha = 1/137.035999679$ .



The largest contribution to the total energy of Eq. (1) comes from the BO component. In order to reach  $10^{-4}$  cm $^{-1}$  accuracy for the energy level, the BO potential converged to at least 11 significant figures has to be generated. Such an accuracy has become available since the recent advent of the analytic integrals over two-center two-electron exponential functions [48]. The BO potential used in the present work has been recently published in Ref. [17]. It was computed using asymptotically correct generalized Heitler-London functions constructed from products of atomic He functions and arbitrary polynomials in interparticle distances

$$e^{-\alpha(r_{1A}+r_{2A})} r_{12}^{n_1} r_{1A}^{n_2} r_{1B}^{n_3} r_{2A}^{n_4} r_{2B}^{n_5}. \quad (32)$$

$\varphi_{\text{el}}(\vec{r})$  expanded in 20 000 such basis functions yielded accuracy of  $10^{-12}$  hartree or even better for large distances [17]. This result is at least four orders of magnitude more accurate than previous values [24, 26, 27, 49]. With this accuracy the error of BO calculations contributes insignificantly to the overall error budget of the dissociation energy.

The electronic wave function  $\varphi_{\text{el}}$  is involved also in evaluation of all the other components of the total energy. However, because so far the analytic integrals in the exponential basis have been unknown, the basis of explicitly correlated Gaussian (ECG) functions has been employed to evaluate the post-BO corrections. The ECG basis functions have the form introduced by Singer [50]

$$\begin{aligned} \psi_k(\vec{r}_1, \vec{r}_2) = & (1 + \hat{P}_{12}) \Xi_k \\ & \times \exp \left[ - \sum_{i,j=1}^2 A_{k,ij} (\vec{r}_i - \vec{s}_{k,i}) (\vec{r}_j - \vec{s}_{k,j}) \right], \end{aligned} \quad (33)$$

where the matrices  $\mathbf{A}_k$  and vectors  $\vec{s}_k$  contain nonlinear parameters, 5 per basis function, to be variationally optimized (see e.g. [51, 52]). The antisymmetry projector  $(1 + \hat{P}_{12})$  ensures singlet symmetry and the  $\Xi_k$  prefactor enforces  $\Sigma$  states when equal to 1, or  $\Pi$  states when equal to  $y_i$ —the perpendicular Cartesian component of the electron coordinate. At short and medium internuclear distances, the accuracy of the BO potential achieved with 3000-term ECG wave functions is  $10^{-9}$  hartree, and with growing  $R$  it gradually decreases. The deterioration of the accuracy at large  $R$ , where the wave function approaches the atomic helium ground state, results from location of the origin of the coordinate system far from the helium nucleus.

All the corrections to BO potential have been evaluated at 70 internuclear distances, including very short ( $R=0.01$ ) and long ( $R=12.0$ ) ones. Subsequently, the potentials involved in the nuclear Schrödinger equation (16) were constructed by interpolation or fitting to these 70 points. Johnson’s solver [53], modified for the variable reduced nuclear mass, was used to obtain the rovibrational levels. Calculations of the second order quantities (Eqs. 20, 21, 23–25, 30) involve additional ECG basis sets (33) employed to inverse the resolvent. For each  $R$  separately, the nonlinear parameters  $\mathbf{A}_k$  and  $\vec{s}_k$  of these basis functions were optimized with respect to a pertinent goal functional (for examples see Table I of Ref. [44] as well as Ref. [54]).

Because, for  $\text{HeH}^+$  the calculations of QED effects have never been done before, we present in Table I numerical values of  $\ln k_0$  and  $\langle \varphi_{\text{el}} | 1/r_{ab}^3 | \varphi_{\text{el}} \rangle_{\text{el}}$  for selected internuclear distances.

At first glance, the calculations on  $\text{HeH}^+$  seem to be very similar to those of the other two-electron molecules studied previously [30–32, 44]. There are however reasons which make these calculations more sophisticated than analogous calculations for  $\text{H}_2$  or HD. First of all, because of the nuclear charge asymmetry, the  $\text{HeH}^+$  molecule is, in contrast to HD, non-symmetric with respect to the inversion of the electronic coordinates in any origin of the coordinate system. The lack of the gerade/ungerade symmetry results in a longer expansion of the BO wave function required to achieve an accuracy similar to that of  $\text{H}_2$ . Such a wave function, in turn, needs more effort in an optimization of the nonlinear variational parameters and is more exposed to linear dependency problem.

Another difference, substantial from the computational point of view, is in the non-symmetric dissociation which is related to the problem of choice of the coordinate system origin. For small and intermediate internuclear distances  $R$ , the reasonable choice of the origin is at the center of the nuclear mass or in the middle of the internuclear distance. Because  $\text{HeH}^+$  decays to the bare proton and the neutral helium atom carrying both electrons, the optimum choice of the origin at large  $R$  is on the helium nucleus. The choice of the origin influences the formulas as well as numerical accuracy of e.g. finite mass corrections. Therefore, to assure the highest possible quality of the calculations, the origin selection issue has to be properly addressed. We coped with this problem by introducing the variable origin nuclear Hamiltonian  $H_n$  of Eq. (8) and a new differential operator  $\vec{\nabla}$ , Eq. (9), which has the property that  $\vec{\nabla}\varphi_{\text{el}}$  is independent of the choice of the origin.

TABLE I: Numerical values of the Bethe logarithm  $\ln k_0$  and the expectation value  $\langle \varphi_{\text{el}} | 1/r_{ab}^3 | \varphi_{\text{el}} \rangle_{\text{el}}$  for selected internuclear distances  $R$ . All entries in a.u.

$R$	$\ln k_0$	$\langle \varphi_{\text{el}}   1/r_{ab}^3   \varphi_{\text{el}} \rangle_{\text{el}}$
Li <sup>+</sup> (1S)	5.179849140 <sup>a</sup>	0.1788 <sup>b</sup>
0.1	4.5407	0.4551
0.5	4.2384	1.3603
1.0	4.2902	1.1715
1.2	4.3123	1.0796
1.4	4.3292	1.0090
1.6	4.3417	0.9632
1.8	4.3506	0.9345
2.0	4.3569	0.9212
2.5	4.3655	0.9262
3.0	4.3687	0.9462
3.6	4.3699	0.9676
He(1S)	4.370160223 <sup>a</sup>	0.989274 <sup>c</sup>

<sup>a</sup> [55], Tab. III;

<sup>b</sup> From 600-term ECG atomic wave function;

<sup>c</sup> [42], Tab. I.

The nuclear charge asymmetry introduces another distinction between HeH<sup>+</sup> and H<sub>2</sub> (or HD). Namely, for HeH<sup>+</sup> the nonadiabatic potentials  $\mathcal{W}_{\parallel}$ ,  $\mathcal{W}_{\perp}$  do not vanish at the united atom limit. Their numerical values depend only on the charges and masses of nuclei and at  $R = 0$  both amount to  $-8.125\,839 \cdot 10^{-9}$  a.u. The long range limits of the nonadiabatic potentials are also known:  $\mathcal{W}_{\parallel}(\infty) = \mathcal{W}_{\perp}(\infty) = -m_e/M_{\alpha}^2 + \mathcal{O}[(m_e/M)^3] \approx -1.879 \cdot 10^{-8}$  a.u.

The nonadiabatic potentials  $\mathcal{W}_{\parallel}(R)$  and  $\mathcal{W}_{\perp}(R)$  are in the following relation

$$\mathcal{W}(R) = \frac{1}{2\mu_n} \frac{m_e}{M_p} g^{\text{el}}(R) \quad (34)$$

with the electronic component of the vibrational and rotational  $g$ -factors appearing in the effective molecular Hamiltonian derived by Herman and Asgharian [56]. For HeH<sup>+</sup> these

$g$ -factor functions have been computed by Sauer *et al.* [19] using a linear response method with full-CI/aug-cc-pVTZ functions. Numerical values reported in [19] have been evaluated using the atomic instead of the nuclear reduced mass. When adjusted to the nuclear reduced mass formalism [57] the  $g$ -factors lead to  $\mathcal{W}$  potentials which differ from ours by only a few percent.

In a molecule, the moving nuclei are "coated" with electrons, bearing additional mass. The amount of the mass changes with  $R$ , which is reflected by the effective nuclear reduced masses  $\mu(R)$  depicted in Fig. 2. Both functions smoothly join the  $\mu(0)$  value

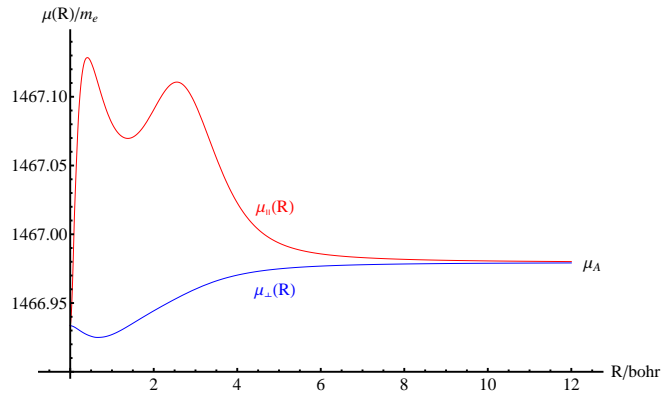


FIG. 2: The  $R$ -dependence of the effective nuclear reduced masses.

with the  $R \rightarrow \infty$  value corresponding to the reduced mass of the separated atoms  $\mu_A = (1/M_p + 1/(M_\alpha + 2m_e))^{-1}$ .

The nonadiabatic effects enter the Schrödinger equation (16) in a twofold way. Firstly, through the variable nuclear reduced masses  $\mu_{\parallel}$  and  $\mu_{\perp}$  described above. Secondly, through the 'nondiagonal' correction  $\delta\mathcal{E}_{\text{na}}$  (Eq. (22)) to the potential  $\mathcal{V}$ . An interesting question arises: what is the effect of neglecting one of these contributions. It turns out that if we omit the contribution from  $\delta\mathcal{E}_{\text{na}}$ , then the nonadiabatic correction to  $D_0$  of the ground rovibrational level amounts to  $0.093 \text{ cm}^{-1}$  which makes 85% of the full correction. Whereas, if we set  $W(R) = 0$ , i.e. if we assume that the nuclear reduced mass is a constant, and if we let  $\delta\mathcal{E}_{\text{na}}$  contribute to  $\mathcal{V}$  then we obtain  $0.017 \text{ cm}^{-1}$  that is 15% of the full correction. As we can see, the contributions are additive and definitely the variable mass contribution is much more significant. The Supplemental Material [58] contains a list of the numerical values of the above mentioned nonadiabatic potentials  $\mathcal{W}_{\parallel}(R)$ ,  $\mathcal{W}_{\perp}(R)$ , and  $\delta\mathcal{E}_{\text{na}}(R)$ , as well as the remaining corrections making the total potential  $\mathcal{V}(R)$ .

Table II collects results for the dissociation energy  $D_0 = E(\text{He}) - E(v = 0, J = 0)$  of the ground rovibrational level. Apart from the total value, this table shows particular components of  $D_0$  obtained within a given level of theory. Each entry is accompanied by an estimated uncertainty resulting from numerical inaccuracy or from neglecting higher order nonadiabatic or QED contributions. We note a significance of the adiabatic correction. In relative numbers this contribution to  $D_0$  is three times larger than in  $\text{H}_2$  with its  $D_0 = 36\,118.0696\text{ cm}^{-1}$  [30]. What is more, it acts in the opposite direction than in  $\text{H}_2$ , that is it decreases the dissociation energy. The leading nonadiabatic correction contribution to  $D_0$  is almost two orders of magnitude smaller than the adiabatic correction and its sign is the opposite. Its value is several times smaller than in  $\text{H}_2$  ( $0.4339\text{ cm}^{-1}$ ) and close to that of  $\text{D}_2$  ( $0.1563\text{ cm}^{-1}$ ), which suggests that at the present level of accuracy the higher order nonadiabatic terms can safely be neglected. The smallness of the nonadiabatic effect can be rationalized by the presence of the heavier nucleus ( $^4\text{He}$ ) and by the observation that the lowest electronic singlet excited state is ca.  $0.4\text{ hartree} = 88000\text{ cm}^{-1}$  above the dissociation threshold of the ground electronic state. This makes the latter to be well isolated from the manifold of the excited states and the nonadiabatic couplings are expected to be small [59]. The relativistic correction to  $D_0$  is close to that found in  $\text{H}_2$  ( $-0.5319\text{ cm}^{-1}$ ) although its relative contribution is significantly larger. The  $\alpha^3$  and  $\alpha^4$  QED contributions remain apparently smaller in both absolute and relative numbers than in the hydrogen molecule.

In the estimation of the uncertainties assigned to the results shown in Table II, we have taken into account two major factors. The first factor is related to the incompleteness of the wave functions employed to evaluate particular expectation values (or the Bethe logarithm) comprising the post-BO corrections. In our calculations, the only quantity computed directly as an expectation value was the orbit-orbit term in the Breit-Pauli Hamiltonian (27). All the other quantities were either the expectation values evaluated using the integral transform technique [64] or second-order quantities, which require the presence of an internal basis set to invert the resolvent. In both cases there are no regular convergence patterns observed usually in the case of the conventional expectation values. It is possible, however, to determine these digits of the numerical result, which remain stable under a change (e.g. doubling) of the basis set size, and assign, with a proper margin of safety, a reliable uncertainty to the evaluated quantity. The second potential source of the error comes from the interpolation of the potentials while numerically solving the radial Schrödinger equation. In our calcu-

TABLE II: Components of  $D_0$  (in  $\text{cm}^{-1}$ ) for the  $v = 0, J = 0$  state of  ${}^4\text{HeH}^+$ . Uncertainties are given in parentheses in units of the last displayed digits.

Component	$D_0/\text{cm}^{-1}$
BO	14 882.154 49(1)
Adiabatic correction	-7.587(3)
Nonadiabatic correction	0.110(2)
$\alpha^0$ subtotal	14 874.677(5)
$\alpha^2$ correction	-0.459(3)
$\alpha^2$ recoil correction	0.000(2)
$\alpha^0 + \alpha^2$ subtotal	14 874.218(10)
$\alpha^3$ correction	-0.00506(2)
$\alpha^4$ correction	0.00029(14)
Total	14 874.213(10)

lations, this source of error has been effectively eliminated by using sufficiently dense grid of computed points—the interpolation uncertainties are negligible in comparison with the errors of individual points of the potentials. Finally, the uncertainty from a component of the potential is transferred to the corresponding correction to  $D_0$ , i.e. its is assumed that the number of significant digits of the correction is the same as that of the potential. We note that the corrections at the separated atoms limit are known exactly and their subtraction introduces no additional error. Just the opposite, it causes a partial error compensation which makes our uncertainties rather overestimated.

Our theoretically predicted  $D_0$  cannot be verified experimentally as no pertinent measurements have been performed yet. It can however be compared with other values predicted theoretically. Of particular interest to us are those calculations which go beyond BO approximation. Bishop and Cheung [27] have reported adiabatic  $D_0 = 14\,873.6\text{ cm}^{-1}$  which appears smaller by  $2.2\text{ cm}^{-1}$  than our adiabatic value. Their adiabatic correction equal to  $-7.6\text{ cm}^{-1}$  agrees well with our prediction. More recently Stanke *et al.* [28] have obtained the nonadiabatic-relativistic energy of the ground level from which the  $D_0 = 14\,873.836\text{ cm}^{-1}$  can be inferred. Again, this value is smaller than our total by  $0.38\text{ cm}^{-1}$ . Stanke *et al.* supply also a purely nonrelativistic energy for this level. Their value  $14874.65351\text{ cm}^{-1}$  is only

by  $0.02 \text{ cm}^{-1}$  smaller than the corresponding ( $\alpha^0$  subtotal)  $D_0$  value of Table II. With increasing vibrational quantum number  $v$  the analogous difference first grows up to  $0.03 \text{ cm}^{-1}$  (for  $v = 2$ ) and then gradually decreases to  $0.002 \text{ cm}^{-1}$  for the highest rotationless state ( $v = 11$ ).

We noticed a significant discrepancy between our relativistic correction to  $D_0$  of  $-0.46 \text{ cm}^{-1}$  and the value of  $-0.82 \text{ cm}^{-1}$  inferred from Stanke *et al.* calculations by subtracting their  $\alpha^2 \langle H_{\text{rel}} \rangle$  from the  $\alpha^2$  correction of He atom [42]. One would expect that a difference in the two methodologically different approaches is attributed to the recoil effect. However, the  $0.36 \text{ cm}^{-1}$  discrepancy is much too large to explain this effect which can be roughly estimated as the relativistic correction divided by the nuclear reduced mass. We gauge that the relativistic recoil contribution to  $D_0$  is less than  $0.002 \text{ cm}^{-1}$  and add this value to the error budget in Table II.

Table III contains dissociation energy of the lowest rovibrational levels ( $v \leq 5$ ,  $J \leq 14$ ) of  $\text{HeH}^+$ . We estimate that uncertainty of the data in Table III is also on the order of  $0.01 \text{ cm}^{-1}$  with a tendency to grow with increasing quantum numbers  $v$  or  $J$ .

For comparison, results of the most accurate experiments undertaken over the years, consisting of about fifty rovibrational transitions, have been assembled together with our theoretical predictions (see Table IV). Among them there are two extremely accurate measurements of  $(0, 0) \rightarrow (0, 1)$  line by Matsushima *et al.* [14] and of  $(0, 1) \rightarrow (1, 2)$  transition by Chen *et al.* [60]. Their uncertainty is of the order of  $10^{-6} \text{ cm}^{-1}$ . The other, older measurements have declared uncertainty of  $0.001 - 0.005 \text{ cm}^{-1}$ . We observe that for most of the line positions the difference between theory and experiment is a few hundredths of inverse centimeter. For about 30 % of the lines the agreement is better than  $0.01 \text{ cm}^{-1}$ .

Stanke *et al.* [61] have performed a fit of the Dunham series to a collection of rovibrational transitions. From this fit they predicted three energy separations between rotationless ( $J = 0$ ) levels:  $2910.9572(7)$  for 0-1,  $2604.1482(12)$  for 1-2, and  $2295.5340(61) \text{ cm}^{-1}$  for 2-3 vibrational band with  $1\sigma$  statistical uncertainty given in parentheses. Differences between our predictions and these Dunham parameters are, respectively:  $-0.005$ ,  $-0.003$ , and  $0.048 \text{ cm}^{-1}$ . Slightly better agreement has been observed for another method of fitting based on Herman-Ogilvie equation [62]. In this case the corresponding discrepancies are  $-0.007$ ,  $-0.002$ , and  $0.002 \text{ cm}^{-1}$ .

## V. CONCLUSION

An accuracy of the order of  $0.01 \text{ cm}^{-1}$  for the theoretically predicted dissociation energy of  $\text{HeH}^+$  has been achieved due to the recent progress made in two directions. The first one, enabled a complete treatment of the leading QED effects. In particular, the approach to effectively calculate the many electron Bethe logarithm and mean values of singular operators, like the Araki-Sucher term, has been developed [30, 63, 64]. The second direction, indispensable to reach this accuracy, is the nonadiabatic perturbation theory (NAPT) [43–45], which enables a rigorous approach to the finite nuclear mass effects beyond the adiabatic approximation.

Uncertainty of our results comes mainly from: (i) the neglect of the finite nuclear mass corrections of the order  $\alpha^2 m/M$  to the relativistic contribution to the PEC; (ii) the

TABLE III: Theoretically predicted dissociation energies (in  $\text{cm}^{-1}$ ) of the lowest bound states of  $^4\text{HeH}^+$ .  $v$  and  $J$  are the vibrational and rotational quantum numbers, respectively.

$J \setminus v$	0	1	2	3	4	5
0	14874.213	11963.261	9359.116	7063.534	5081.451	3421.052
1	14807.165	11901.648	9302.983	7012.996	5036.712	3382.432
2	14673.455	11778.802	9191.091	6912.293	4947.616	3305.592
3	14473.856	11595.477	9024.185	6762.171	4814.924	3191.330
4	14209.515	11352.795	8803.374	6563.743	4639.773	3040.844
5	13881.942	11052.236	8530.122	6318.477	4423.672	2855.735
6	13492.995	10695.621	8206.235	6028.196	4168.502	2638.009
7	13044.861	10285.098	7833.849	5695.060	3876.506	2390.089
8	12540.035	9823.124	7415.413	5321.560	3550.297	2114.837
9	11981.297	9312.442	6953.676	4910.514	3192.859	1815.586
10	11371.691	8756.066	6451.672	4465.056	2807.564	1496.200
11	10714.501	8157.259	5912.711	3988.647	2398.204	1161.181
12	10013.224	7519.518	5340.369	3485.077	1969.045	815.856
13	9271.556	6846.561	4738.489	2958.500	1524.925	466.731
14	8493.367	6142.313	4111.190	2413.482	1071.426	122.261



approximate treatment of the  $\alpha^4$  correction; (iii) the neglect of higher order nonadiabatic terms proportional to  $(m/M)^3$ .

### Acknowledgments

This research was supported by the NCN grant N-N204-015338, by a computing grant from Poznań Supercomputing and Networking Center, and by PL-Grid Infrastructure.

- 
- [1] S. Lepp, P. C. Stancil, and A. Dalgarno, *J. Phys. B* **35**, R57 (2002).
  - [2] S. Lepp, *Astrophys. Space Sci.* **285**, 737 (2003).
  - [3] P. C. Stancil, S. Lepp, and A. Dalgarno, *Astrophys. J.* **509**, 1 (1998).
  - [4] C. Cecchi-Pestellini and A. Dalgarno, *Astrophys. J.* **413**, 611 (1993).
  - [5] I. Rabadán, B. K. Sarpal, and J. Tennyson, *Mon. Not. R. Astron. Soc.* **299**, 171 (1998).
  - [6] I. Dabrowski and G. Herzberg, *Top. N.Y. Acad. Sci.* **2** **38**, 14 (1977).
  - [7] J. H. Black, *Astrophys. J.* **222**, 125 (1978).
  - [8] W. Roberge and A. Dalgarno, *Astrophys. J.* **255**, 489 (1982).
  - [9] V. P. Gaur, G. C. Joshi, and M. C. Pande, *Bull. Astron. Soc. India* **20**, 217 (1992).
  - [10] B. Zygelman, P. C. Stancil, and A. Dalgarno, *Astrophys. J.* **508**, 151 (1998).
  - [11] M. Larsson and A. E. Orel, *Dissociative Recombination of Molecular Ions* (Cambridge University Press, 2008).
  - [12] A. Saenz, *Phys. Rev. A* **67**, 033409 (2003).
  - [13] J. Purder, S. Civiš, C. Blom, and M. van Hemert, *J. Mol. Spectrosc.* **153**, 701 (1992).
  - [14] F. Matsushima, T. Oka, and K. Takagi, *Phys. Rev. Lett.* **78**, 1664 (1997).
  - [15] M. W. Crofton, R. S. Altman, N. N. Haese, and T. Oka, *J. Chem. Phys.* **91**, 5882 (1989).
  - [16] J. A. Coxon and P. G. Hajigeorgiou, *J. Mol. Spectrosc.* **193**, 306 (1999).
  - [17] K. Pachucki, *Phys. Rev. A* **85**, 042511 (2012).
  - [18] T. A. Green, H. H. Michels, J. C. Browne, and M. M. Madsen, *J. Chem. Phys.* **61**, 5186 (1974).
  - [19] S. Sauer, H. Jensen, and J. Ogilvie, *Adv. Quantum Chem.* **48**, 319 (2005).

- [20] J. Loreau, J. Lievin, P. Palmeri, P. Quinet, and N. Vaeck, *J. Phys. B* **43**, 065101 (2010).
- [21] C. A. Coulson and W. E. Duncanson, *Proc. R. Soc. Lond. A* **165**, 90 (1938).
- [22] A. A. Evett, *J. Chem. Phys.* **23**, 1169 (1955).
- [23] J. Goodisman, *J. Chem. Phys.* **43**, 3037 (1965).
- [24] L. Wolniewicz, *J. Chem. Phys.* **43**, 1087 (1965).
- [25] W. Kolos, *Int. J. Quantum Chem.* **10**, 217 (1976).
- [26] W. Kolos and J. Peek, *Chem. Phys.* **12**, 381 (1976).
- [27] D. M. Bishop and L. M. Cheung, *J. Mol. Spectrosc.* **75**, 462 (1979).
- [28] M. Stanke, D. Kędziera, S. Bubin, and L. Adamowicz, *Phys. Rev. A* **77**, 022506 (2008).
- [29] B. J. Drouin, S. Yu, J. C. Pearson, and H. Gupta, *J. Mol. Struct.* **1006**, 2 (2011).
- [30] K. Piszczatowski, G. Lach, M. Przybytek, J. Komasa, K. Pachucki, and B. Jeziorski, *J. Chem. Theory Comput.* **5**, 3039 (2009).
- [31] K. Pachucki and J. Komasa, *Phys. Chem. Chem. Phys.* **12**, 9188 (2010).
- [32] J. Komasa, K. Piszczatowski, G. Lach, M. Przybytek, B. Jeziorski, and K. Pachucki, *J. Chem. Theory Comput.* **7**, 3105 (2011).
- [33] A. Campargue, S. Kassi, K. Pachucki, and J. Komasa, *Phys. Chem. Chem. Phys.* **14**, 802 (2012).
- [34] J. Liu, E. J. Salumbides, U. Hollenstein, J. C. J. Koelemeij, K. S. E. Eikema, W. Ubachs, and F. Merkt, *J. Chem. Phys.* **130**, 174306 (2009).
- [35] D. Sprecher, J. Liu, C. Jungen, W. Ubachs, and F. Merkt, *J. Chem. Phys.* **133**, 111102 (2010).
- [36] J. Liu, D. Sprecher, C. Jungen, W. Ubachs, and F. Merkt, *J. Chem. Phys.* **132**, 154301 (2010).
- [37] P. Maddaloni, P. Malara, E. D. Tommasi, M. D. Rosa, I. Ricciardi, G. Gagliardi, F. Tamassia, G. D. Lonardo, and P. D. Natale, *J. Chem. Phys.* **133**, 154317 (pages 4) (2010).
- [38] S. Kassi and A. Campargue, *J. Mol. Spectrosc.* **267**, 36 (2011).
- [39] S.-M. Hu, H. Pan, C.-F. Cheng, Y. R. Sun, X.-F. Li, J. Wang, A. Campargue, and A.-W. Liu, *Astrophys. J.* **749**, 76 (2012).
- [40] W. E. Caswell and G. P. Lepage, *Phys. Lett. B* **167**, 437 (1986).
- [41] K. Pachucki, *Phys. Rev. A* **71**, 012503 (2005).
- [42] K. Pachucki, *Phys. Rev. A* **74**, 022512 (2006).
- [43] K. Pachucki and J. Komasa, *J. Chem. Phys.* **129**, 034102 (2008).
- [44] K. Pachucki and J. Komasa, *J. Chem. Phys.* **130**, 164113 (2009).

- [45] K. Pachucki, Phys. Rev. A **81**, 032505 (2010).
- [46] I. Sick, Phys. Rev. C **77**, 041302 (2008).
- [47] <http://www.physics.nist.gov/cuu/Constants>.
- [48] K. Pachucki, Phys. Rev. A **80**, 032520 (2009).
- [49] W. Cencek, J. Komasa, and J. Rychlewski, Chem. Phys. Lett. **246**, 417 (1995).
- [50] K. Singer, Proc. R. Soc. Lond. A **258**, 412 (1960).
- [51] J. Komasa and A. J. Thakkar, Chem. Phys. Lett. **222**, 65 (1994).
- [52] J. Komasa, Phys. Chem. Chem. Phys. **10**, 3383 (2008).
- [53] W. R. Johnson, *Atomic Structure Theory*, Lectures on Atomic Physics (Springer-Verlag, Berlin and New York, 2007).
- [54] J. Komasa, Phys. Rev. A **65**, 012506 (2001).
- [55] V. A. Yerokhin and K. Pachucki, Phys. Rev. A **81**, 022507 (2010).
- [56] R. Herman and A. Asgharian, J. Mol. Spectrosc. **19**, 305 (1966).
- [57] S. P. A. Sauer (2011), private communication.
- [58] See supplementary material at [URL] for a list of the numerical values of all the potentials.
- [59] A. Carrington, R. A. Kennedy, T. P. Softley, P. G. Fournier, and E. G. Richard, Chem. Phys. **81**, 251 (1983).
- [60] H.-C. Chen, C.-Y. Hsiao, J.-L. Peng, T. Amano, and J.-T. Shy, 66-th International Symposium of Molecular Spectroscopy, 20-24 June 2011, Ohio.
- [61] M. Stanke, D. Kędziera, M. Molski, S. Bubin, M. Barysz, and L. Adamowicz, Phys. Rev. Lett. **96**, 233002 (2006).
- [62] R. M. Herman and J. F. Ogilvie, Adv. Chem. Phys. **103**, 187 (1998).
- [63] K. Pachucki and J. Komasa, J. Chem. Phys. **124**, 064308 (2006).
- [64] K. Pachucki, W. Cencek, and J. Komasa, J. Chem. Phys. **122**, 184101 (2005).

TABLE IV: Comparison of theoretical predictions with available measured line positions (in  $\text{cm}^{-1}$ ) of  $v''-v'$  vibrational bands in  $^4\text{HeH}^+$ .

Transition	Theory	Experiment	Difference	Reference
0-0				
R(0)	67.0488	67.052517(7)	-0.0037	Matsushima 1997
R(1)	133.7097	133.716942(6)	-0.0072	Matsushima 1997
R(6)	448.1342	448.160(3)	-0.026	Liu 1987
1-0				
P(1)	2843.9033	2843.9035(20)	-0.0002	Bernath and Amano 1982
P(2)	2771.8065	2771.8059(20)	0.0006	Bernath and Amano 1982
P(3)	2695.0540	2695.0500(20)	0.0040	Bernath and Amano 1982
P(4)	2614.0384	2614.0295(20)	0.0089	Bernath and Amano 1982
P(5)	2529.1474	2529.134(5)	0.013	Crofton 1989
P(6)	2440.7597	2440.742(5)	0.018	Crofton 1989
P(9)	2158.1731	2158.140	0.033	Purder 1992
P(10)	2059.2496	2059.210	0.040	Purder 1992
P(11)	1958.4351	1958.388	0.047	Purder 1992
P(12)	1855.9652	1855.905(2)	0.060	Tolliver 1979
P(13)	1752.0375	1751.971(2)	0.066	Tolliver 1979
R(0)	2972.5650	2972.5732(20)	-0.0082	Bernath and Amano 1982
R(1)	3028.3626	3028.374869(7)	-0.0123	Chen 2011
		3028.3750(20)	-0.0124	Bernath and Amano 1982
R(2)	3077.9782	3077.9919(20)	-0.0137	Bernath and Amano 1982
R(3)	3121.0612	3121.0765(20)	-0.0153	Bernath and Amano 1982
R(4)	3157.2795	3157.2967(20)	-0.0172	Bernath and Amano 1982
R(5)	3186.3215	3186.337(5)	-0.016	Crofton 1989
R(6)	3207.8970	3207.909(5)	-0.012	Crofton 1989
R(7)	3221.7372	3221.752(5)	-0.015	Crofton 1989
2-1				
P(1)	2542.5328	2542.531(1)	0.002	Blom 1987
		2542.534(5)	-0.001	Crofton 1989
P(2)	2475.8194	2475.814(1)	0.005	Blom 1987
		2475.815(5)	0.004	Crofton 1989
P(5)	2248.8616	2248.854	0.008	Purder 1992
P(6)	2165.4987	2165.485	0.014	Purder 1992
P(7)	2078.8630	2078.841	0.022	Purder 1992
P(8)	1989.2748	1989.251	0.024	Purder 1992
P(9)	1897.0290	1896.992(2)	0.037	Tolliver 1979
P(10)	1802.3900	1802.349(2)	0.041	Tolliver 1979
P(11)	1705.5869	1705.543(2)	0.044	Tolliver 1979
R(0)	2660.2787	2660.284(1)	-0.005	Blom 1987
R(1)	2710.5578	2710.556(1)	0.002	Blom 1987
		2710.563(5)	-0.005	Crofton 1989
R(2)	2754.6173	2754.624(5)	-0.007	Crofton 1989
R(3)	2792.1027	2792.110(5)	-0.007	Crofton 1989
R(4)	2822.6728	2822.683(5)	-0.010	Crofton 1989
R(5)	2846.0003	2846.009(5)	-0.009	Crofton 1989
R(6)	2861.7716	2861.786(5)	-0.014	Crofton 1989
R(7)	2869.6854	2869.69	-0.005	Crofton 1989
R(8)	2869.4483	2869.478(5)	-0.030	Crofton 1989
3-2				
P(5)	1966.3794	1966.356	0.023	Purder 1992
R(4)	2484.8965	2484.912	-0.015	Purder 1992
R(5)	2501.9260	2501.941	-0.015	Purder 1992
R(6)	2511.1758	2511.188	-0.012	Purder 1992
R(8)	2504.8992	2504.914	-0.015	Purder 1992
R(9)	2488.6192	2488.632	-0.013	Purder 1992